Available online at www.sciencedirect.com

ScienceDirect

Advances in Space Research 60 (2017) 652–666

ADVANCES IN SPACE RESEARCH (a COSPAR publication)

www.elsevier.com/locate/asr

A seasonal study on the role of h'F/meridional winds in influencing the development of ESF irregularities over Indian sector

Sreeba Sreekumar, S. Sripathi *

Indian Institute of Geomagnetism, Navi Mumbai, India

Received 10 October 2016; received in revised form 7 April 2017; accepted 10 April 2017
Available online 20 April 2017

Abstract

In this paper, we present the seasonal variation of nighttime thermospheric meridional winds over Hyderabad as derived using dual ionosonde observations located at Tirunelveli (8.7°N, 77.7°E, Dip Lat = 0.3°N), an equatorial station and Hyderabad (17.38°N, 78.45°E, Dip Lat = 12°N), a low latitude station, respectively, over the period of April-December 2013 using h'F data as discussed in (Sreekumar and Sripathi, 2016). The calculated winds has been compared with HWM14 wind model. The results show that trends of the derived winds from the ionosonde h'F data matches well with model wind near to midnight hours in all the seasons. However, some dissimilarities were observed during early night hours. Especially, the poleward winds during early night hours for different seasons were not well reproduced by the model. Later, the study is extended to understand the role of meridional winds in causing the variability of ESF occurrence vis a vis h'F. The histogram analysis of h'F vs wind values just before ESF onset reveals that the most probable combination of wind and h'F on the ESF days are centered around 350 km and 50 m/s. Additionally, we also performed Superposed Epoch Analysis (SEA) based on longer and shorter duration ESF events. The analysis reveals the distinct differences in the longer and shorter duration ESF events of Summer and Autumn equinox where the values of h'F as well as meridional winds where such that a steep change in reduction of poleward winds prior to ESF onset supported the longer duration ESF events in both seasons. However, this steep reduction is not so significant for the shorter duration ESF events indicating that meridional winds could play a crucial role in extending the spread F durations in longer duration events. The observations clearly demonstrate the reduction of poleward wind velocities during vernal equinox as compared to Autumn equinox, where larger poleward winds were present around ESF onset times. These observations are consistent with the equinoctial asymmetry as seen during year 2013 where more number of ESF occurrences were observed during vernal equinox as compared to Autumn equinox. Additionally on seasonal basis, analysis of the significance of meridional wind magnitudes during scintillation and non scintillation days were performed. The result suggests that non scintillation days were characterized with larger poleward wind magnitudes than scintillation days during vernal equinox and summer season. However, such a trend was not seen in the Autumn equinox season. This might indicate the possible role of poleward meridional wind in reducing the number of scintillation occurences during this season in addition to weakening of PRE height.

Keywords: ESF irregularities; Meridional winds and h'F

1. Introduction

The evening equatorial ionosphere is a platform for the generation of various electrodynamical processses in the equatorial F region. One among them is the phenomenon of equatorial spread F(ESF) which is characterized by density irregularities. These irregularities are believed to drastically affect the radio commmunication and navigation systems. Day to day variabilities of ESF is still a major concern in ionospheric research. The basic generation mechanism of ESF is due to the action of Rayleigh Taylor

* Corresponding author.
E-mail address: ssripathi.iig@gmail.com (S. Sripathi).

http://dx.doi.org/10.1016/j.asr.2017.04.009
0273-1177/

(RT) instability operating under certain conditions. These favourable condition occurs during the post sunset hours. However, various other background parameters like accelaration due to gravity, plasma density gradient scale length, F region base height h'F, ion-neutral collision frequency and gravity waves have a major say in enhancing the growth rate of RT instability. During the post sunset hours, under the action of recombination and due to the enhancement of eastward electric fields (PRE) through F region dynamo process, the F layer will be raised to higher altitudes. This corresponds to a region of lesser ion neutral collision frequency values and thereby RT instability can operate efficiently. Hence, all these processes contribute to ESF generation. Further, the eastward zonal wind in the presence of a westward density gradient and vertically downward wind in the presence of an upward density gradient are also equally important in the ESF development.

However, to trigger RT instability, seeding is required in the bottomside of the F region. Using Jicamarca radar maps, Kelley et al. (1981) reported that gravity waves act as seed perturbations. More recently, Manju et al. (2016) reported that the amplitude of the gravity wave seed perturbation is a very critical parameter which decides whether or not ESF would occur on a given day. However, Kudeki et al. (2007) concluded that equatorial post-sunset bubble generation should not be critically dependent on gravity-wave seeding – instead the critical factor seems to be the eastward wind. Chum et al. (2016) studied the horizontal velocities of spread F structures seen by multipoint continous Doppler sounding over Tucuman, Northern Argentina and over Taiwan. They attributed the observed oblique Spread Structures(OSS) to the equatorial/low latitude spread F and roughly eastward propagation in both Tucuman and Taiwan. Further, using ionosonde data from two stations in Brazillian sector, de Abreu et al. (2014b) and de Abreu et al. (2014a) discussed the role of planetary waves(PW) in affecting the day to day variability of ESF. They concluded that, in the F region day to day variations, signatures of PWs with several day periods were present. This suggests the modification of PRE by PWs and thereby causing the generation of medium and large scale irregularities.

The interrelation among various factors assisting/suppressing ESF has been mentioned in Abdu (2005). One among the candidates is the thermospheric meridional/trans-equatorial winds and their role(positive/negative influences) in causing the day to day variability of ESF as mentioned in the previous papers (Maruyama, 1988; Sultan, 1996; Devasia et al., 2002; Abdu et al., 2006; Huba and Krall, 2013). Maruyama (1988) showed that poleward meridional winds can push the ionization down to the E region and thereby stabilize the ionosphere. This lead to an enhancement in the E region conductivity, thereby reducing the F region dynamo and PRE development. Thus eventually reducing the F region height rise. While, equatorward meridional winds can raise the F layer to higher altitudes. The effect of large poleward winds is that they can move the F layer to lower altitudes, where ionization loss due to recombination is more prominent. Using ionosonde data from SHAR and Trivandrum, Krishna Murthy et al. (1990) adopted a method to obtain the nighttime thermospheric meridional winds over SHAR. The method has been later validated by Sekar and Sridharan (1992) using high-altitude vapour releases from SHAR. Further, using this method, relationship between h'F vs meridional winds on the occurence of ESF has been reported by Devasia et al. (2002). They reported that for the equinoctial period, equatorward winds are a must for the occurence of ESF, when h'F is less than 300 km. Also, Jyoti et al. (2004) concluded that, for lower F layer heights over Trivandrum, equatorward winds could contribute to bottomside spread F. Maruyama et al. (2009) reported, using numerical simulations of plasma bubble development, included trans equatorial wind effects which suggested that, on changing the wind velocity from 10 to 40 m/s, the growth time of bubble also reduced to half.

The seasonal behaviour of meridional neutral winds were reported by Hari and Murthy (1995). Recently, Madhav Haridas et al. (2013) has studied the seasonal and solar activity variations of threshold height needed for ESF occurence irrespective of the polarity of the meridional winds. However, this study was carried out for non ESF days of disturbed periods. As far as Indian sector is concerned, not many reports are in the literature which brings out the impact of meridional winds vs h'F on spread F generation, particularly covering all seasons. Hence our attempt in understanding of the same can be helpful in giving some insight into the problem of ESF variabilities.

Present study evolves as an extension of our previous work (Sreekumar and Sripathi, 2016) which was focussed on the estimation and comparison of meridional winds as well as their role in ESF development/suppression, during vernal equinox (March-April) season during the year 2013. However, the contribution of h'F and meridional wind towards the day to day variabilities in ESF generation during other seasons also needs to be evaluated. Hence the present work deals with an attempt to understand how the factors such as h'F and meridional winds affect the ESF generation/suppression during different seasons. In this regard, as a supportive analysis, Superposed Epoch Analysis(SEA) technique has been perfomed. Further various aspects regarding the importance of h'F and meridional winds in the development of ESF irregularities/scintillations has been carried out. The details of the study will be discussed in the subsequent sections.

2. Data and methods of analysis

The meridional wind estimations used in this study involves the use of the method mentioned in Krishna Murthy et al. (1990). The main essence of this method is as follows: At night time, the vertical drift at the equator will be only due to electrodynamic drift (E*X*B drift), but for stations slightly away from the equator, the vertical drift will be affected by diffusion along the field lines as well as due to meridional winds. In this method, we have derived the night time thermospheric meridional winds over Hyderabad using h'F values obtained from two ionosondes. One is located in the equatorial region Tirunelveli (8.73°N, 77.7°E, Dip Lat = 0.3°N) and other station, Hyderabad (17.38°N, 78.45°E, Dip Lat = 12°N) which is slightly away from the equator. Hereafter, the equatorial station, Tirunelveli is denoted as TIR, whereas the low latitude station, Hyderabad is denoted as HYD. Thus meridional winds are having significant influence over low latitude stations and their influence depends on the dip angle (inclinaton angle), 'I' of the region. i.e., low latitude station should have higher dip latitude value which comes in the range of 8–15° will be sufficient for meridional wind influence to be noted (Krishna Murthy et al., 1990). Hence Hyderabad station is suitable for estimating winds using this method. The h'F values from the ionograms over TIR and HYD has been scaled for 4 and 4.5 MHz frequencies. Hence the errors can be minimized at these lower frequencies. This has been done so as to reduce the error in further calculations. The time resolution of the h'F data of both stations are of ten minutes. It is to be noted that data analyzed in this study is restricted only to geomagnetically quiet days. To serve the purpose, we have selected the quiet days with a criterion of Ap index <15.

The basic equations used in the estimation of meridional winds are as follows: The time rate of change of virtual height of F layer, i.e., Vertical drift velocity

$$V_o = \frac{d(h'F)}{dt} \tag{1}$$

The vertical drift, $\frac{d(h'F)}{dt}$ has been obtained for two frequencies 4 and 4.5 MHz for each stations. The electrodynamic drift at Tirunelveli(TIR) and Hyderabad (HYD) is denoted as V_T and V_H

$$V_T = V_{oT} - \beta_{oT} H_{oT} \tag{2}$$

$$V_H = V_{oH} - \beta_{oH} H_{oH} \tag{3}$$

V_{oT} and V_{oH} denotes the vertical drift at TIR and HYD and β_{oT} and β_{oH} are the effective chemical loss coefficients (attachment coefficient) at TIR and HYD. The ionization scale heights, H_{oT} and H_{oH}, obtained at the heights of reflection at 4 and 4.5 MHz has been considered for both stations. It is assumed that E X B drift is the same over both stations, TIR and HYD. As the stations are not largely seperated, this assumption is valid. Hence according to this, any change in the electric field E, with dip in the region covering the two stations are omitted. Also, further the difference in longitude between the two stations is <1°. This implies that both stations are located on the same meridian, which thereby ensures that any change in V_T and V_H within this longitude value at the same local time is neglected.

Additionally, when h'F is at lower altitudes, the term β_{oT} and β_{oH} represent the apparent effects in the vertical drift velocity due to chemical loss. Hence, as mentioned by Bittencourt and Abdu (1981), 300 km is used as threshold height to calculate such apparent velocities in V_T and V_H. The terms β_{oT} and β_{oH} are obtained from the following equation

$$\beta = K_1(N_2) + K_2(O_2) \tag{4}$$

where β represents the effective chemical loss coefficients. K_1 and K_2 are the temperature dependent reaction rates involving N_2 and O_2. (N_2) and (O_2) represents the number densities of N_2 and O_2, respectively, which are obtained from MSIS-E-90 model. Both K_1 and K_2 are obtained from Anderson and Rusch (1980) and given as:

$$K_1 = 2 * 10^{-11} * \left(\frac{T_n}{300}\right)^{-1/2} \tag{5}$$

$$K_2 = 1 * 10^{-10} \tag{6}$$

and are expressed in cm^3/s. T_n is the neutral temperature as obtained from MSIS-E-90 model.

The Ionization Scale height, H is given as,

$$H = \left(\frac{1}{N} * \frac{dN}{dH}\right)^{-1} \tag{7}$$

where N is the background electron density.

The horizontal component of the thermospheric neutral wind aligned with the geomagnetic field is given as U_m. i.e.,

$$U_m = 2\left(\frac{V_T \cos I - V_H}{\sin 2I}\right) - W_D \tan I \tag{8}$$

Here the meridional winds, U_m are estimated over HYD station. I denotes the inclination angle. H is Ionization Scale height. W_D is the plasma diffusion drift term is given by Rishbeth et al. (1978) and can be obtained from the vertical plasma drift velocity at F2 peak as,

$$V_{zm} = W - \left(\frac{g}{v_m}\right)\sin^2 I = W - \left(\frac{D_m}{2H}\right)\sin^2 I \tag{9}$$

Here, W is the vertical plasma drift applied to the layer by wind/electric field. D is the plasma diffusion coefficient given by

$$Dv = 2gH \tag{10}$$

Hence, on rearrangement,

$$W_D \tan I = \frac{g}{v_{in}} \tan(I) \tag{11}$$

g and v_{in} denotes the acceleration due to gravity and ion neutral collision frequency respectively. Here v_{in} is obtained from Banks and Kockarts (1973) and is given as,

$$v_{in} = 2.6 \times 10^{-9} \times (N_2) \times sqrt\left(\frac{\alpha_{O\_N_2}}{\mu_1}\right) + (O_2) \times sqrt\left(\frac{\alpha_{O\_O_2}}{\mu_2}\right) + (O) \times sqrt\left(\frac{\alpha_{O\_O}}{\mu_3}\right) \tag{12}$$

$\alpha_O\_N_2, \alpha_O\_O_2$ and α_O_O denotes the polarizability of O_N_2, O_O_2 and O_O respectively. μ_1, μ_2 and μ_3 represents the reduced masses of O+ and N_2, O+ and O_2 and O+ and O.

The study also presents Superposed Epoch Analysis (SEA), a technique which consists of sorting data into different categories and comparing their means. The method is also known as compositing. The main principle of the technique is that on averaging the data in a proper way, in relation to the event, the event signal will be remained. Also, all other influences will undergo averaging. i.e., in brief, the data sequence can be broken into different sets of equal duration and all the sets can be made to superpose. As a first step, the data is categorized with equal durations and then mean of each section is obtained. Thus for a sufficient data, common response to an event should emerge in the form of average. However, the noise in the data will be cancelling out. The technique is commonly used for identifying the behaviour of geomagnetic storms.

In the present study, for each ESF event, we divide the category of both meridional wind and h'F into ten minute duration prior to and after 1 hr of the ESF onset. The ESF onset on each day is considered as time = 0. Therefore, estimated wind and h'F values are categorized into an hour before and after the ESF onset including the onset. Hence in this case, a total of 13 classifications will be emerging. Eventually, once these categorization is done, the mean of each category is obtained and this averaged value under each category will be shown in the figures. Hence this analysis helps to understand h'F and wind variations within that particular period of ESF onset, before an hour and after an hour to the onset. This analysis is useful in interpreting the meridional wind and h'F variations around the time of ESF onset and can be valuable in evaluating the plausible importance of each of the parameter discussed in contributing to ESF generation.

2.1. GPS scintillation data

Often, electron density irregularities in the ionospheric region results in degradation of the radio wave signals causing fluctuations in amplitude and phase of the signal received at the reciever. In order to measure the amplitude scinillations, S4 index is a widely used parameter which is obtained as the normalized standard deviation of the intensity of the recieved signal power. In our study, we use GPS L band (L1 frequency at 1.57542 GHz) amplitude scintillation data as obtained from Tirunelveli (equatorial station) for studying GPS scintillations and its duration. Only those events, whose duration is above 0.5 hr were considered as scintillation days, while duration lesser than this value were considered as non scintillation days.

2.2. HWM14 model

The meridional neutral winds obtained in the present study is compared with the new Horizontal Wind Model 14 (HWM 14) (Drob et al., 2015). The model is an improved version of older models like HWM93 and HWM 07 and provides an improved observationally based, time-dependent, global empirical specification of the upper atmospheric general circulation patterns and migrating tides. HWM provides a reliable reference for the validation of general circulation models. While there are lesser changes incorporated in the HWM14 model for lower altitudes, significant improvements are made in the upper thermosphere portion (above 120 km).

3. Observations and results

In this work, we present and discuss the analysis of association of h'F/meridional wind during spread F vs non spread F days during the year 2013. We have considered Summer (May-Aug), Autumn equinox (Sep-Oct) and winter (Nov-Dec) months for the study. Due to data gap, we have not considered January-February months. For comparison purposes, we will be using some data from Vernal equinox (Apr). The results of which have been presented previously in our companion paper (Sreekumar and Sripathi, 2016). By convention, meridional wind directions in the northern hemisphere are positive for poleward (northward) winds and negative for equatorward (southward) winds. Further, the average values of solar flux (for the days considered here) for Vernal equinox, Summer, Autumn equinox and Winter are 119.3, 117.2, 102.4, 146.1 Solar Flux Unit (SFU), respectively for the year 2013.

3.1. Seasonal variation of night time meridional winds using h'F data method

Here, we present a few examples of meridional wind variation on ESF and non ESF days from each season. In Fig. 1, we present typical examples of meridional wind variations during ESF (panel (a)) and non ESF (panel (b)) days during Summer season. Panel (a) in Fig. 1 gives the h'F (km), vertical drift (m/s) and meridional wind (U_m, m/s) variation for May 29–30, 2013 a spread F day (Ap = 1). Blue and red horizontal bars in the upper panel of the figure indicates the spread F duration over TIR and HYD respectively. Bottom panel shows the h'F values at TIR and HYD in blue and red colour curves respectively, the middle panel gives the vertical drift, dh'F/dt for both stations. Top panel gives meridional winds estimated over HYD as derived from h'F data at the two stations (TIR and HYD), by including necessary corrections for plasma diffusion and chemical recombination.

Initially, it is evident that the h'F values at both stations are well below 300 km. However, after ~1930 LT, h'F at HYD reaches ~305 km. h'F at TIR is still below 300 km. The wind variations are such that the poleward wind in the early evening period reaches a maximum at 1840 LT, begins to reduce and temporarily reaches the largest equatorward velocities by 1930 LT. The ESF over TIR started at 1920 LT and continued till 2230 LT, followed by the occurence at 0200–0500 LT. A steep change from poleward to equatorward velocities is seen at 1900 LT. The winds

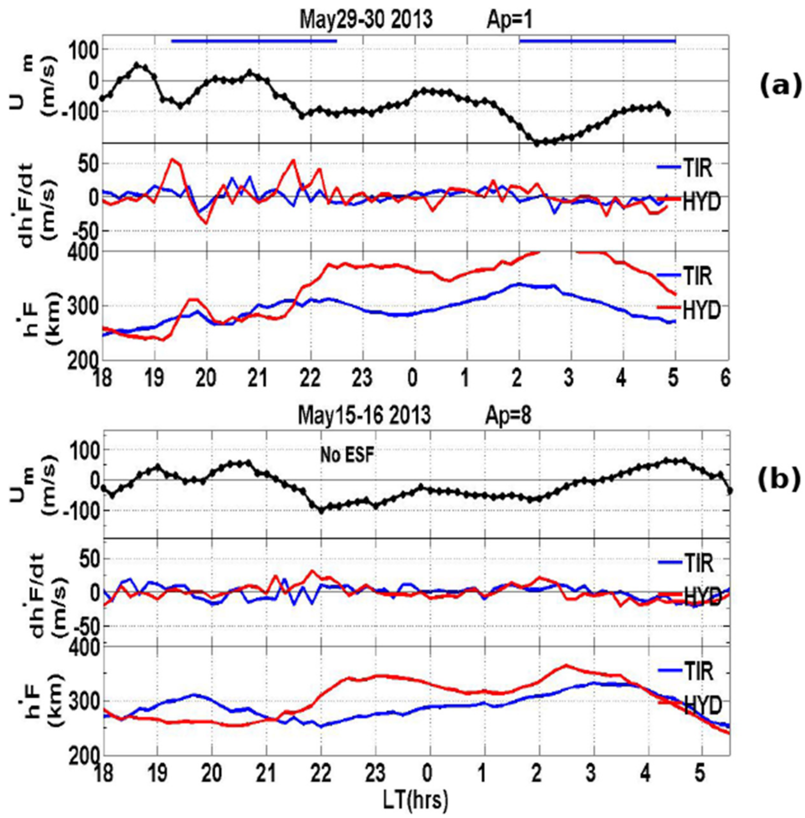

Fig. 1. The top figure is a case study showing the variation of h'F (bottom panel), dh'F/dt (middle panel) and meridional wind (top panel) for May 29–30, 2013 (Ap = 1, Spread F day); The bottom figure is for May15–16, 2013 (Ap = 8), Non Spread F day.

were equatorward from 1900 to 2000 LT. The winds were predominantly equatorward from 2100 LT onwards. It can be also seen that spread F was absent over HYD during the whole period.

Panel (b) in Fig. 1 shows the h'F, vertical drift and wind variation for May 15–16, 2013, a non spread F day (Ap = 8). Although the overall wind pattern remained more or less same as in the previous case, one can notice that poleward wind velocity reaches a local maximum by 1900 LT. Further, the reduction in poleward wind values occur which is not so prominent (less steep) as compared to the previous case. h'F values at TIR around the period almost reaches 300 km by 1900 LT unlike the previous one. However, spread F is seen to be absent over both the stations. The wind directions were predominantly equatorward from 2120 LT till 0300 LT and became poleward thereafter.

In Fig. 2, we present typical examples of meridional wind variations during ESF (panel (a)) and non ESF (panel (b)) days during Autumn equinox season. Panel (a) in Fig. 2 depicts the meridional winds estimated during September 13–14, 2013 (Ap = 9). The equatorward wind at 1800 LT, turns poleward with maximum poleward velocities reached at 1900 LT. This was followed by a reduction in poleward wind velocities and reached equatorward for a shortwhile. By 2000 LT, wind turn poleward for about an hour. After 2100 LT, the wind remained equatorward. h'F at TIR was ~350 km. ESF at TIR started by 1930 LT and remained till 0400 LT. HYD spread F got initiated by 2220 LT.

Panel (b) in Fig. 2 represents a non spread F day, Sep 3–4, 2013 (Ap = 6). Winds were poleward from 1800 to 1910 LT. However, the poleward velocities reduced after 1830 LT. Steep change in poleward to equatorward wind is less visible. i.e.,the reversal to equatorward values were slower than the earlier case. It is observed that ESF was absent on this day. The wind reaching an equatorward minimum at ~0000 LT, afterwards started to increase the equatorward velocities.

In Fig. 3, we present typical examples of meridional wind variations during ESF (panel (a)) and non ESF (panel (b)) days during Winter season. Panel (a) in Fig. 3 denotes the winds estimated during December 29–30, 2013 (Ap = 4). Wind velocities were predominantly poleward from 1830 to 0010 LT. The local maximum of poleward velocity was reached at 1840 LT. Although slight reduction in poleward wind amplitudes occur at 1850 LT, thereby reaching an amplitude of ~80 m/s. The ESF began at TIR by 1900 LT and sustained till 0300 LT. HYD spread F started by 1950 LT and was of short duration. h'F value was 400 km at 1900 LT. Accordingly, vertical drift values were ~40 m/s around that time. Further increase in poleward values was seen by 2130 LT. At 0000 LT, the directions were reversed to equatorward for a short while. It

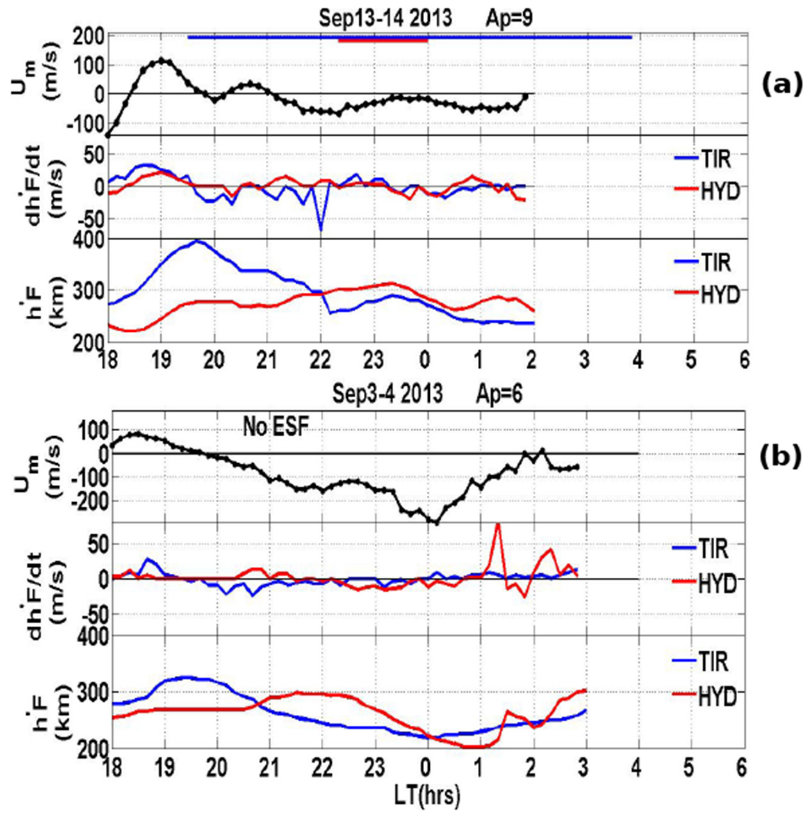

Fig. 2. The top figure is a case study showing the variation of h'F (bottom panel), dh'F/dt (middle panel) and meridional wind (top panel) for September 13–14, 2013 (Ap = 9, Spread F day); (b) The bottom figure is for September 3–4, 2013 (Ap = 6, Non Spread F day).

can be understood that, h'F value of ~400 km by 1900 LT, as well as the reduction of poleward wind velocities just before ESF onset might have assisted in ESF formation in this case.

Panel (b) in Fig. 3 shows another case on December 6–7, 2013, a non spread F day. The h'F values were 360 km by 1900 LT. Wind values were consistently poleward during the post sunset hours till 2030 LT. By 1940 LT, poleward wind values reduced. For a shortwhile, wind became equatorward at 2100 LT. At 2200 LT, wind became poleward for a while, followed by equatorward turning. Afterwards, it remained equatorward for two hours followed by poleward velocities at 0100 LT.

3.2. Winds obtained from h'F data method vs HWM14 model

Fig. 4 shows the mean meridional winds (U_m) over HYD derived using (a) HMM14 model and (b) h'F method during Apr-Dec 2013. It is seen that the wind magnitudes obtained using both method and model show significant differences. However, the equatorward trend of U_m during the late night hours is evident from both (a) and (b). This is consistent in all the seasons except for some differences during winter season. However, to understand the generation/day to day variability of ESF, the study mainly focuses on the early night hours during these seasons. During 1800–2000 LT period, the vernal equinox season is seen to have HWM14 winds mainly poleward with lesser magnitudes. h'F method also gives poleward winds, with comparatively greater poleward wind magnitudes. During Summer months, h'F derived winds are characterized by equatorward to poleward transition during post sunset hours, contrary to that the model winds are poleward to equatorward during these hours. The increased poleward magnitudes during 1900–2100 LT for Jun-Aug is not reproduced well in the model. Contrary to that, equatorward winds are seen in the model wind. During Sep-Oct, h'F derived winds are having reversals from poleward to equatorward direction for Oct cases, while Sep data shows an equatorward to poleward reversal. Morever, during post sunset hours, the poleward magnitudes are comparatively larger for Oct case. HWM14 model winds do not show this difference during Sep months. Instead, they are reversing from poleward to equatorward values unlike h'F wind. During Oct period, the higher poleward values are seen in the early half, which is reproduced well in model case. However, with lesser wind values compared to h'F case. Also, their reduction to equatorward direction occurs slightly late than in other seasons. During winter, we could not include more number of days due to lack of simultaneous data at both stations. However, winter season wind seems to have higher poleward values both in model and derived one. Higher values being in the case of h'F derived wind. A major difference in the wind pattern during Oct and Nov is the higher poleward wind values during 2100–2300 LT

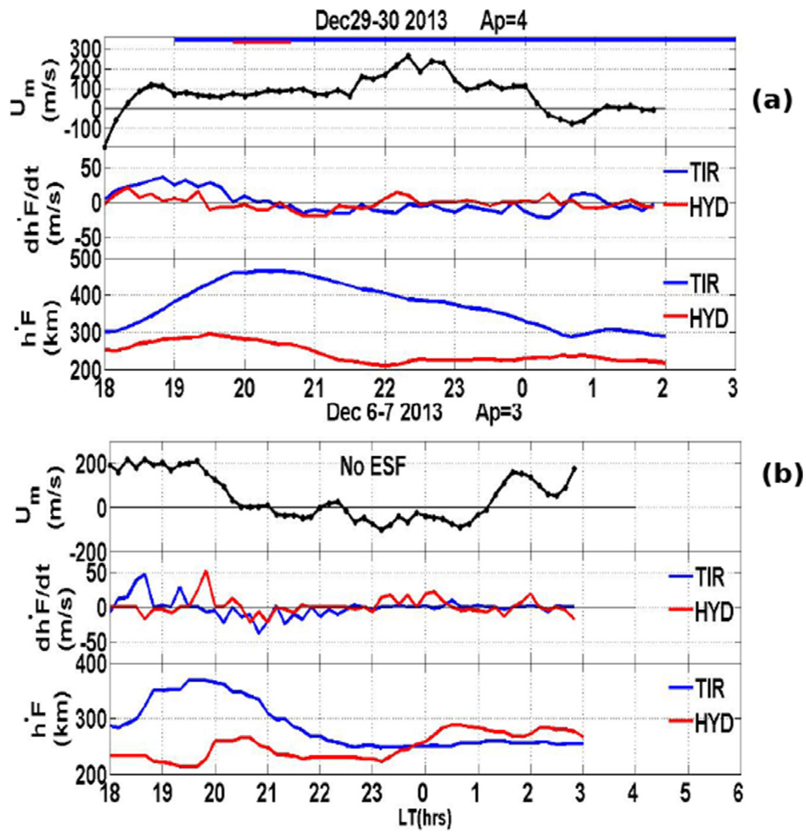

Fig. 3. (a) A case study showing the variation of h'F (bottom panel) dh'F/dt (middle panel) and the meridional wind (top panel) for December 29–30, 2013 (Ap = 4, spread F day); (b) for December 6–7 (Ap = 3, Non spread F day).

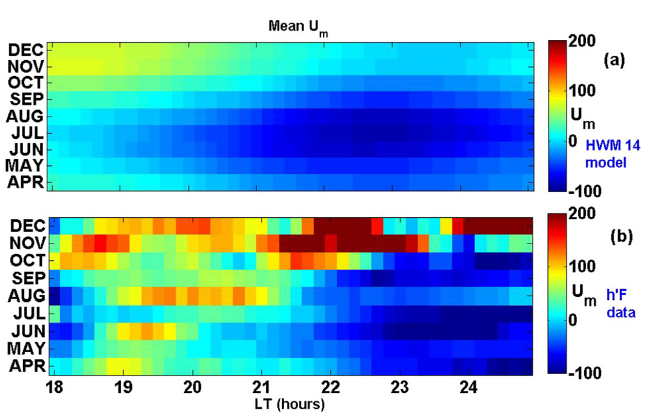

Fig. 4. (a) Winds during ESF days obtained using HWM14 model for the season from April-December. (b) The winds derived using h'F data.

which is not reproduced in the model winds. Hence it is evident that both similarities as well as dissimilarities can be inferred from model and h'F derived wind.

Fig. 5(a)–(c) shows the mean values of wind derived using h'F data for ESF days during Summer (May-Jun-Jul-Aug, denoted as MJJA), Autumn equinox (Sep-Oct or SO) and Winter period (Nov- Dec or ND) respectively. The individual days used for each seasons are shown in light blue colour, whereas the average values and standard deviations are denoted in red colour. During MJJA, although, the poleward wind magnitudes are reduced by 1930 LT, the wind values are poleward in the pre midnight hours till 2100 LT. After 2100 LT, wind became equatorward and remained so. Likewise, the average wind values for September-October shows mainly poleward values till 2200 LT. The mean wind values during Nov-Dec shows predominantly poleward magnitudes with comparatively larger values. Additionally, the wind values show clear oscillations throughout the period. After 0130 LT, wind became equatorward.

3.3. Salient features of meridional winds/h'F on ESF vs non ESF days

Fig. 6 gives the temporal variation of mean winds during ESF vs non ESF days during 2013 obtained using h'F method. Fig. 6(a) denotes ESF days during Apr-Dec. Since there were no non ESF days in other months, only May-Sep and Dec is considered for non ESF case. The white portion during Apr, Oct and Nov indicates absence of non ESF cases. It is seen from Fig. 6(a) that the average pattern of wind during Apr is such that although the wind is poleward by 1900 LT, afterwards its reduction occured. However Sep cases show that winds reduced their equatorward velocities before 1900 LT and by 1900 LT became poleward. However, a slight difference is found during October. The winds were poleward before 1900 LT and

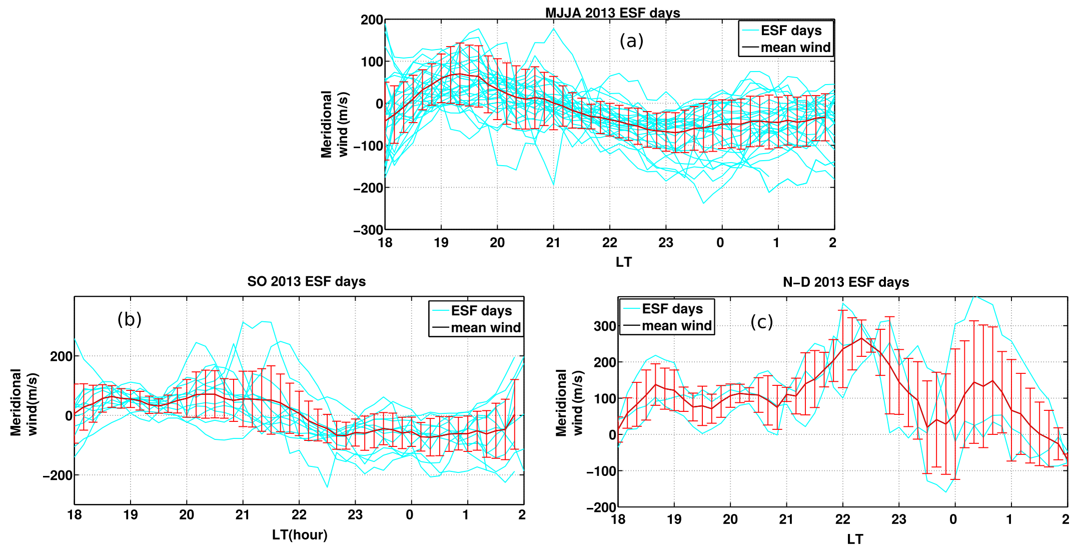

Fig. 5. Seasonal average of meridional wind on ESF days for the year 2013 (a) for May-August(MJJA), (b) for September-October(SO) and (c) November-December(ND). All the ESF days are shown in light blue curves, thick red line gives the average value of wind, Standard deviations are also shown along with them. (For interpretation of the references to colour in this figure legend, the reader is referred to the web version of this article.)

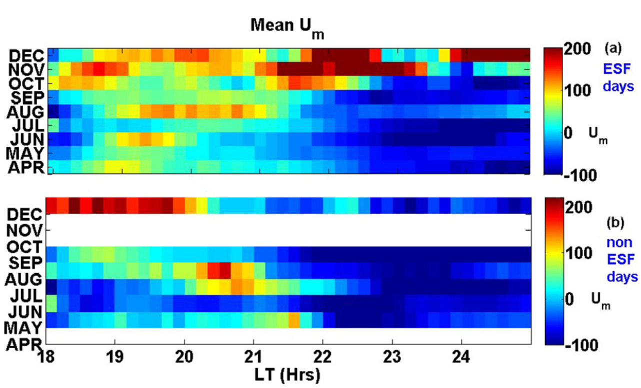

Fig. 6. Plot showing the mean wind values on (a) ESF vs (b) Non ESF days for all the months considered.

their poleward magnitudes reduced just after 1900 LT. During Nov-Dec, winds were strongly poleward by 1900 LT. May-Jun-Jul-Aug seasons were having equatorward velocities during early sunset hours, however, with a clear poleward wind turning by 1900 LT. Analysis of non ESF cases are presented in Fig. 6(b). Here, considering MJJA season, presence of strong poleward wind magnitudes around 2000–2200 followed by equatorward wind velocities are noted. During Sep, increase in poleward wind magnitudes by 1900 LT is noted. Also, it is evident that during Dec, large poleward wind magnitudes are present around 1900 LT.

Fig. 7 presents the mean value of h'F at TIR for (a) ESF vs (b) non ESF days. During ESF days, around 1800–1900 LT, Apr, Oct and Nov-Dec season have higher values of h'F. In addition, the peak value of h'F occurs earlier in Nov. Further on comparing Apr and Sep equinox period, maximum h'F reaches early for Sep cases. The summer solstice from May-Aug shows lower h'F values during 1800–1900 LT. However, after 1900 LT, May and August are having higher h'F values. During non ESF days (as shown in (b)), while May-Jul have low values of h'F during post sunset hours, Aug-Sep and Dec shows comparatively higher h'F values around the same period. A comparison of ESF vs non ESF days, show that higher values of h'F are clearly evident during ESF days than non ESF days of Apr, Sep-Oct and Nov-Dec.

Fig. 8 gives the mean h'F at HYD during ESF (a) and non ESF day (b) for the different seasons considered. The main difference in this figure is the comparatively higher h'F values near to the midnight hours of May-August during both cases (a) and (b). Further, this h'F value is larger in ESF cases than in non ESF Case. It is seen that the differences between ESF and non ESF case during the month of Sep is such that around 2300–2400 LT, the h'F values are higher for ESF than non ESF events.

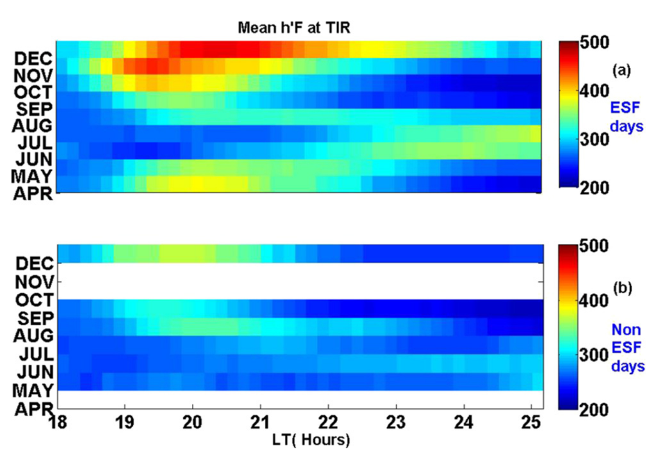

Fig. 7. Plot showing the mean values of h'F at Tirunelveli(TIR) on (a) ESF and (b) Non ESF days.

Fig. 9 shows the histogram plot of h'F vs meridional wind, just before ESF onset during all the seasons. This represents the probability of events occuring under specific conditions. Colour bar indicates the No. of events. It can be seen that majority of the events are centered around wind values of 50 m/s and h'F values of 350 km. Also, some interesting cases of exceptions are also obtained. i.e., A few events were such that the wind values are equatorward, while h'F values were less than 300 km. At the same time, other few events were also seen such that winds were highly poleward, but the h'F values were above 300 km. In between there comes the section in which both meridional wind and h'F contributions are both important for the ESF generation.

Fig. 10 shows the mean value of foF2 crest to trough ratio obtained as foF2(HYD)/foF2(TIR), during (a) ESF days and (b) non ESF days. The white portion in the figure represents the absence of non spread F days during the period considered. Upon considering May-Sep period in both contours, one can observe that FoF2 ratio during ESF days are higher than those on non ESF days. Especially, June, Aug and Sep shows this clear distinction features. i.e., at 1900 LT period, average crest to trough value on ESF cases on July is ~1.1, while it is ~1 during non ESF case. However, the difference is not so large. Similarly, near to 1900 LT hours, Sep seasons shows larger foF2 ratio of ~1.1 than the case ~1 in non ESF days. Further, during Sep also such an enhancement in FoF2 ratio is clearly evident in ESF than on non ESF case. Although there are slight increase in ESF than non ESF days, the difference is not so significant.

Figs. 11 and 12 depicts the Superposed Epoch Analysis (SEA) carried out on ESF days with a classification of short duration (less than or equal to 5 hr) and long duration (>5 hr) for summer and Autumn equinox seasons respectively. Here the winds shown are over HYD, and h'F is estimated over TIR. Due to the limited number of short duration ESF days, this technique is not applied for other seasons. However the long duration cases studied on the same showed steep reduction in poleward values of wind. The details of this technique is already discussed in previous section. Zero marks the ESF onset time and hence before and after 'zero' denotes the time before and after the onset. Interestingly, we could note that the longer duration events were characterized by higher h'F values when compared to short duration events. i.e., maximum h'F value reached on ESF days on an average were 380 km and deviations include them to be greater than 400 km. In contrast, the average maximum h'F on short duration events were 320 km and the deviations can go up to 360 km. Similarly, the meridional wind velocities on longer duration ESF days were such that a steep reduction in poleward values can be seen, while on the shorter duration cases, there is no steep change in reduction of poleward values. This is one of the unique result of the study.

Fig. 13 gives a picture of the mean winds during scintillation vs non scintillation days during (a) Vernal equinox (b) Summer and (c) Autumn equinox. The blue and red curve shows the scintillation and non scintillation days respectively. Corresponding standard deviations are shown along with it. Fig. 13(a) has been reproduced from the previous companion paper. During vernal equinox, around 1900 LT, poleward wind velocities increase for non scintillation days. In contrast, reduction in poleward magnitudes

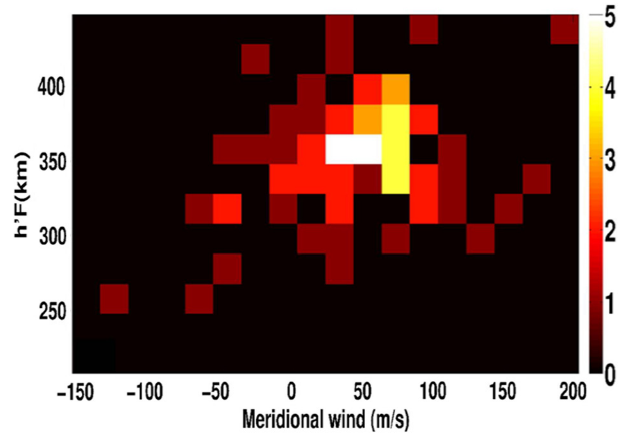

Fig. 9. Histogram plot of h'F vs meridional winds just before ESF onset.

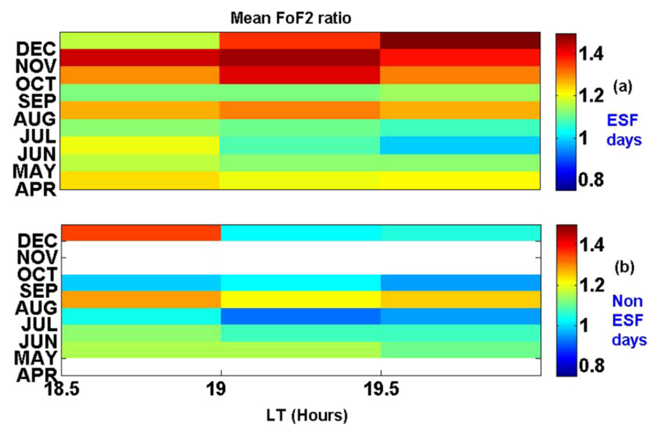

Fig. 10. Mean FoF2 ratio on (a) ESF Days and (b) Non ESF Days.

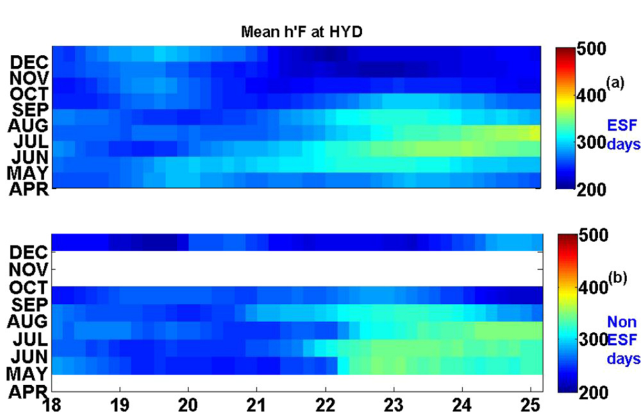

Fig. 8. Plot showing the mean values of h'F at Hyderabad(HYD) on (a) ESF and (b) Non ESF days.

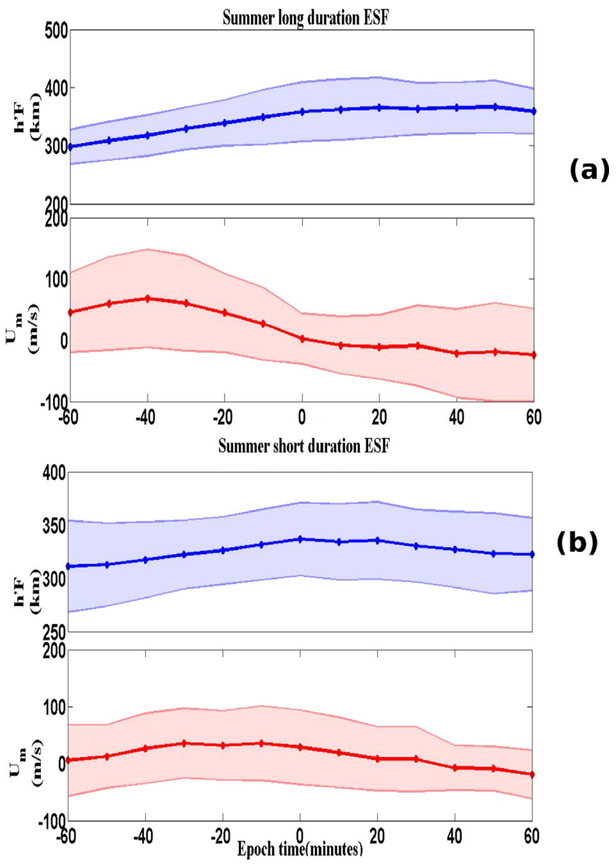

Fig. 11. h'F vs meridional wind an hour before and after ESF onset (a) For Summer long duration ESF events and (b) For Summer short duration ESF events.

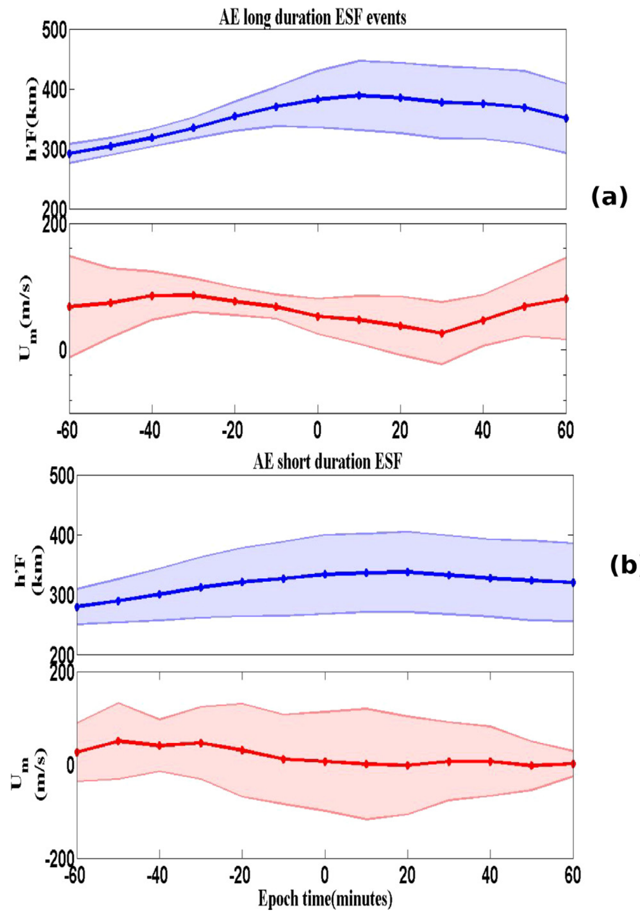

Fig. 12. h'F vs meridional wind an hour before and after ESF onset (a) For Autumn equinox long duration ESF events and (b) For Autumn equinox short duration ESF events.

occur for scintillation days. During MJJA, the poleward winds increase for non scintillation days around 1900 LT; while the poleward winds reach maximum and start decreasing for scintillation days around 1900 LT. Also, the figure shows that during both seasons, higher poleward wind velocities are observed on non scintillation cases, as compared to scintillation days. However during SO, at post sunset hours, around 1900 LT, although poleward wind velocities are visible on non scintillation days, they are smaller than on scintillation days.

4. Discussions

Present study deals with the analysis of the characteristics of meridional wind and h'F during ESF and non ESF days. As a part of the study, we compared the winds estimated using h'F data with the recent HWM14 model. Comparison of derived winds and HWM14 winds shows that both are best matched near the late night hours during ESF days. It is observed that, near post midnight hours, where the prominence of equatorward velocities are noted, the model reproduced the calculated winds very well. However considering the early night hours, during the seasons, many similarities as well discrepancies were obtained. The important point to note is the differences in wind magnitudes from both results suggest that calculated winds were having higher magnitudes than the model wind. According to seasonwise classification, although higher in magnitudes, in both cases early night (1800–1900 LT) winds are largely poleward during Oct-Nov period. The increase in poleward values at 2000–2300 LT during the same season is however not reproduced by the model wind. Similarly, poleward values during early night hours (1900–2100 LT) of Jun-Aug is not showing similarities with model wind. While comparing model and calculated winds, the similarities/dissimilarities during different seasons have been reported by a few of the previous workers. A recent study by Haridas et al. (2016) report that equatorward nature of winds during summer and poleward winds during winter is reproduced well by HWM model. However, in the calculated winds, the errors can occur from differences in obtaining the h'F values as well as due to errors from diffusion term. Also, the neutral temperature values obtained from MSISE model could also be a source of error and hence the recombination coefficient β.

Regarding the seasonal variation of meridional/transequatorial winds, it is noteworthy to mention some of the previous studies. The meridional winds over a low latitude station, SHAR were estimated by Hari and Murthy (1995)

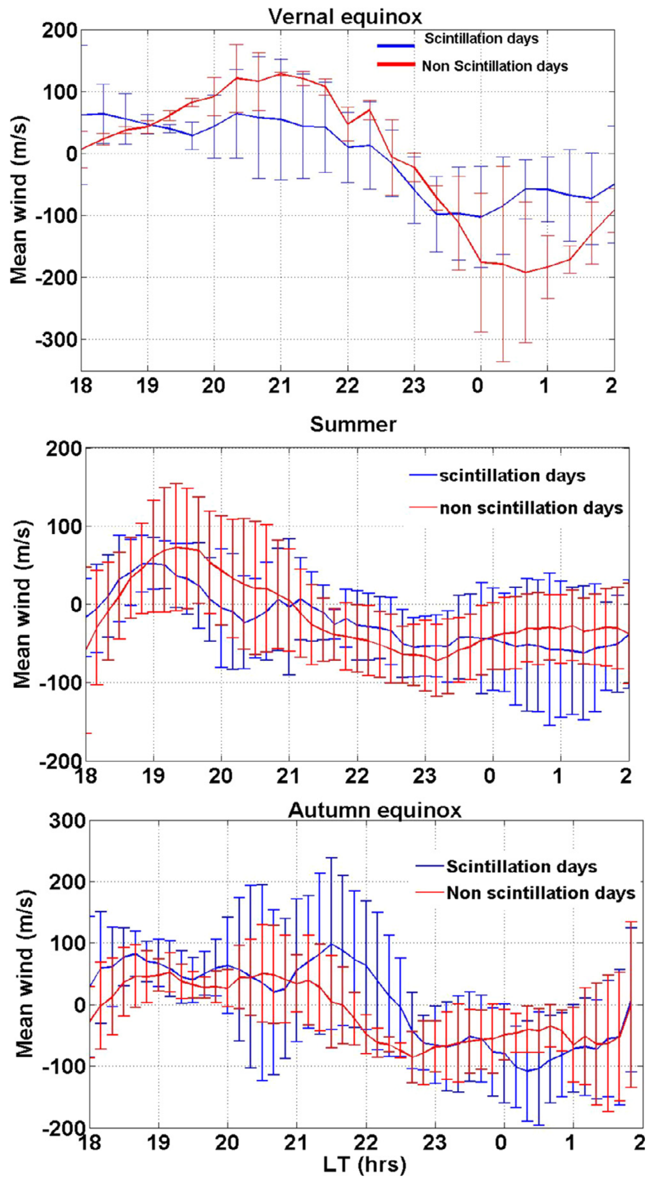

Fig. 13. Mean wind vs time for scintillation vs non scintillation days during(a) Vernal equinox, (b) Summer and (c) Autumn equinox 2013. Blue curve denotes the scintillation days and red denotes the non scintillation days. (For interpretation of the references to colour in this figure legend, the reader is referred to the web version of this article.)

using h'F method from ionosondes located at Trivandrum (equatorial station) and SHAR. They brought out various features of winds during different seasons during non ESF days. They pointed out that value of poleward wind in the early night hours is greatest in winter and least in summer, with equinox wind values being moderate. During a study using the African sector (Ouagadougou), Oyekola (2009) observed that in the evening hours, northward transequatorial wind is larger within the December solstice, moderate in equinoxes and weaker during June solstice. Our results are in accordance with these works.

Further, more recently, during non ESF days, Haridas et al. (2016) investigated the seasonal behaviour of winds during low and high solar activity periods. The seasonal study of vertical winds has been done by Liu et al. (2003) using ionosondes located over Wuhan, China. Furthermore, using ionosonde network of three stations over south east Asia (Maruyama et al., 2008), estimated the thermospheric meridional winds and suggested that the amplitude of the higher order variations was prominent in the winter months of northern hemisphere. This was attributed to the pressure bulge associated with the Midnight Temperature Maximum (MTM). A part of present work includes the comparison of meridional winds during different seasons for ESF as well as non ESF days. Prominent poleward velocities are found in all seasons during non ESF days than ESF cases. Winter (Dec) is showing larger poleward wind magnitudes than other seasons with non ESF days is observed to have larger poleward values. During summer (MJJA), there is larger poleward wind values during 2000–2200 LT.

However, on correlating the wind values with h'F variations over TIR (Fig. 7) for corresponding seasons during ESF and non ESF days reveal interesting features. It is observed that during Winter (Nov), although increase in poleward wind is evident over the season, the increased h'F values over TIR might be associated with presence of ESF during the season. Similarly, Autumn equinox(Sep-Oct) seasons, though not largely poleward as compared to winter months, still shows prominent poleward magnitudes around 1900 LT. Again, increased h'F values are clearly visible over the period as compared to May-Jul. During Summer(May-Jul), during early night hours h'F values are lesser and poleward wind magnitudes are seen during 1900 LT. However, Summer season is believed to have more post midnight occurences of ESF unlike other seasons. Hence, it is seen from the Figs. 6 and 7 that there is an increment in h'F values near midnight hours associated with equatorward wind magnitudes around the same period during ESF days. This might suggest an increase in RT instability as the height is increased which means the F layer is taken to higher altitudes, thus favouring RT instability and generation of irregularities. Contrary to that, although there is equatorward wind present over the midnight hours, non ESF Days are not seen to have an increment in h'F and hence this possibly imply the absence of ESF during those events. Due to the lack of non ESF events during April, the comparison of the same is not presented here. Similarly, Sep-Oct and Nov-Dec seasons have very few non ESF days obtained in the study due to data gap and disturbed conditions. However, analyzing a very few non ESF events vs ESF during Sep indicates that around 1900 LT, poleward wind values are larger during non ESF than ESF events. Although the h'F values are nearly ∼300 km and 350 km for non ESF vs ESF cases respectively, the strong polewards winds during non ESF cases on Sep compared to ESF cases might reveal the absence of ESF on those days.

Another interesting feature to look into will be the equinoctial asymmetry in the ESF occurences as well as the asymmetry in winds. The year 2013 is observed to have more number of ESF cases during Vernal equinox as compared to Autumn equinox cases. Our study indicates that although h'F values are larger around 1900 LT, for these cases during Sep-Oct, the presence of larger poleward winds during these hours might suggest the absence of ESF (Fig. 6(a) and Fig. 7(a)) and hence lesser No.of ESF events during Sep-Oct as compared to Apr. Using the chain of ionosondes situated near the magnetic conjugate points at Chiang Mai, Thailand (18.8 °N, 98.9°E; 13.0° magnetic latitude) and Kototabang, Indonesia (0.2°S, 100.3°E; −10.0° magnetic latitude) and third station situated near the magnetic equator at Chumphon, Thailand (10.7°N, 99.4°E; 3.3° magnetic latitude), Maruyama et al. (2009) pointed out the equinoctial asymmetry in meridional winds. They reported that northward meridional wind was increased and values were larger at Sep equinox than that of Mar equinox. Our study also shows the presence of this feature, as we can see the increased poleward wind magnitudes during Sep than Apr events. Hence, the larger northward wind velocity and lesser ESF occurrence in September as compared with March were consistent with the results of Maruyama et al. (2009) and Maruyama and Matuura (1984) which suggests the suppression of RT instability by the trans equatorial winds. Additionally, the equinoctial asymmetry in the scintillation occurrence in the Indian sector has been examined by Sripathi et al. (2011) and they suggested that asymmetry in electron density and meridional neutral winds as the possible reason for equinoctial asymmetry.

Present study also suggests that the most probable combination of wind and h'F on ESF days were centered around 350 km and 50 m/s. A few events were noted under the category such that even though the height was less, but winds were equatorward which might have assisted spread F generation. Likewise another type events were such that, heights were high, but poleward winds were present. Here the greater heights might have played a dominant role in ESF generation. During the study from Indian sector, Devasia et al. (2002) pointed out that polarity of the winds does not affect ESF generation/suppression until and unless the h'F < 300 km. i.e., when h'F < 300 km, equatorward winds are a must so as to have any influence on ESF. Irrespective of the magnitude and direction of meridional winds, the seasonal/magnetic activity dependence/solar activity of critical height for the ESF occurence has been mentioned in some of the earlier works (Jyoti et al., 2004; Manju et al., 2007; Madhav Haridas et al., 2013). Also, although mainly focussing on the disturbed days of low and high solar active epochs, the seasonal and solar activity variations of the threshold height on ESF occurrence irrespective of the meridional wind polarities are discussed by Madhav Haridas et al. (2013). They suggested that significant modulation of threshold height occurs by O/N_2 changes irrespective of season, solar activity or magnetic activity. However, one of the early studies of effects of meridional winds on ESF occurrence, was given by Maruyama (1988). His study suggested that for a uniform, trans equatorial meridional wind can enhance the field line integrated conductivity and hence promote the reduction of growth rate of generalized RT instability. Using Brazilian sector data, Abdu et al. (2006) reported meridional winds can negatively effect ESF development by reducing the PRE and as a result direct suppression of the RT instability growth rate. However, using NRL 3D equatorial spread F code SAMI3, Huba and Krall (2013) concluded that a wind profile with a positive gradient may show a negative influence on generalized RT instability, while wind profile with a negative gradient can have a positive effect on instability. During a study of numerical simulations of plasma bubble developments, Maruyama et al. (2009) included the transequatorial neutral wind effect and reported that when the velocity of wind increased from 10 to 40 m/s, the growth time (e-folding time) of the bubble was halved.

It is well known that RT instability acting in the bottomside of F region is the basic mechanism for ESF generation. Growth rate of RT instability is understood to be influenced by the asymmetry in Equatorial Ionization Anomaly (EIA) between the two hemispheres. It has been reported by Maruyama and Matuura (1984) that transequatorial winds cause redistibution of ionization with respect to magnetic equator leading to asymmetries in the crests of EIA. Raghavarao et al. (1993) suggested the formation of a meridional circulation cell, as a result of the upward winds over the anomaly crest region and downward winds in the trough region. Consequently, the pressure ridges formed on both sides of the equator due to equatorial temperature and wind anomaly(ETWA) will cause a circulation with the return flow situated in the lower thermospheric regions. Further, the strong converging equatorward winds associated with the EIA, will cause the generation of downward vertical winds over dip equator, hence increasing the possibilities of ESF generation.

As mentioned above, meridional/trans equatorial winds can cause asymmetry in the EIA structure. The value of FoF2 ratio between crest and trough regions can be considered as an indicator of EIA strength. Hence, in an attempt to understand the behaviour of the meridional winds in causing EIA asymmetry, the FoF2 ratio between HYD and TIR is calculated for the different seasons considered in the study. Interestingly, around 1800–1900 LT, an enhancement in the FoF2 $[(HYD)\ /\ (TIR)]$ ratio was visible over Jul, Aug and Sep-Oct periods on ESF days corresponding to their counterparts on non ESF events. Although the calculation shows that the difference between ESF and non ESF cases were not very significant. The most probable reason could be due to the large differences in distance between HYD and crest region. i.e, HYD is a station far from the anomaly crest region. As a result of this, we may not be able to see the enhancements in electron density (FoF2 ratio) to a great extent as it would be over the crest regions. However, for better understanding of the consequences of EIA asymmetry by winds, one needs to use a station as near to the crest of the anomaly. Raghavarao et al. (1988) reported that associated with vertical E X B drift around dip equator, a strong trans equatorial wind can result in a significant asymmetry in the northern and southern EIA crest amplitudes especially during winter. This can act as a condition less favourable for spread F initiation. In this study, it is clearly visible that during winter, around 1900 LT period, there is an increment in the h'F values over TIR as well as HYD.

Another important classification of present work is based on the duration of ESF events. Hence, upon classifying into longer and shorter duration ESF events during Summer and Autumn equinox seasons, SEA is performed. The results focus mainly just before and at ESF onset times and indicate that longer duration ESF events were characterized with steep reduction of poleward wind velocities. Also, it is noticed that h'F values are also assisting this with larger values. However short duration cases were observed with characteristics that there is not much steep change in reduction of poleward velocities. Further h'F values were smaller compared to ESF cases. Based on a campaign data, Sridharan et al. (2014) showed that when h'F at 1930 LT was around 310 km, scintillations lasted for shorter duration, while in the cases for h'F was greater or lesser than the above value, the duration was found to be more. They attributed this to be due to the exponential increase of ion-neutral collision frequency. The variation of the ESF duration during different geophysical conditions were studied by Sreeja et al. (2009) and they reported that the estimation of the duration of ESF on a day can be done by using geomagnetic Kp index and post sunset vertical drift.

Ultimately, from application point of view, the day to day variability of scintillations need to be carefully addressed. Scintillations, with its sufficient intensity can reduce the signal quality, thereby causing severe effects on navigation and communication purposes. Strong amplitude scintillations are produced as a result of largely irregular plasma. Since the understanding of day to day variabilities of scintillations/ESF are of great importance, it is important to know the factors affecting day to day variabilities of them. Here, while analyzing the effect of meridional wind on generation/suppression of scintillations during different seasons, it is observed that the winds during vernal equinox and summer months are such that during non scintillation days, they were more poleward (poleward magnitudes) were larger than scintillation days. The trend is clearly evident in both of these seasons. However, it is noticed that, during autumn equinox season, such an increase in poleward wind during non scintillation days are not visible. In fact, around 1900 LT, the poleward magnitudes are higher on scintillation days than non scintillaton cases. The plausible reason for this might point to the importance of h'F, more than meridional winds during this particular season as can be inferred from Fig. 7. Valladares et al. (2002) reported that the average meridional wind measured either south or north of Arequipa during mid evening hours on scintillation days are more equatorward than those observed on the nights during no scintillations. He also suggests that during winter solstice, no difference in the meridional wind speeds was noted. Our results are consistent with this particular finding, i.e., during vernal, autumn equinox and summer periods, scintillation days are marked by a reduction in poleward wind in the early night hours while non scintillation days show an evident increase in the poleward magnitudes. Although this is the case, it is observed that during Sep-Oct seasons, the meridional wind transitions from poleward to equatorward are not so prominent and hence it can be stated that h'F could be playing significant role in these occassions. As seen from Fig. 7, the h'F values at TIR are quite high compared to other seasons. This might indicate the importance of h'F/PRE for ESF generation over these months. A study by Muella et al. (2010) by using Brazilian stations, mentioned that larger poleward wind magnitudes can suppress the Equatorial Plasma Bubble (EPB) development, by controlling the flux tube integrated conductivities, which can reduce the non linear growth of irregularities.

Present study focussed mainly on the importance of h'F/meridional wind in causing variabilities in ESF over different seasons. Other parameters, i.e., gravity waves, planetary waves, field line integrated conductivities etc. controlling the day to day variablities of ESF are not included in this study. These factors should be also included while considering the day to day variabilities. Hence, the same will be covered as an aspect in our future work. Additionally, at present we do not have wind measurements from other instruments to validate our results. However, in future depending on the availability of the wind measurements, we would like to compare the ionosonde derived winds for validation purposes.

5. Conclusions

We studied the seasonal variation of meridional winds during ESF/non ESF days for the year 2013 using dual ionosonde stations over Indian longitude to understand the role of meridional winds and h'F on the ESF occurence. The main points emerged in the study are as follows:

(1) The comparision of h'F derived winds with that of HWM14 wind model suggest that model winds show similar trends as seen in the observations especially the dominance of equatorward velocities in the late night hours in all the seasons. However, there exists some differences in the magnitude in all seasons where model winds show lesser values as compared to calculated winds.
(2) The seasonal variation of average nighttime thermospheric meridional winds suggests that (a) Autumn equinox have more poleward wind velocities than vernal equinox during post sunset hours; However, large temporal variations is noticed as compared to other seasons. (b) Winter months is seen to have lar-

ger poleward velocities during early night hours compared to all other seasons. (c) However, Summer values being moderate between these two seasons.

(3) SEA obtained for long and short duration events during Summer and Autumn equinox seasons show that the during longer duration events, there was an increase in h'F as well as steep change in the reduction of poleward wind values. The shorter duration events were characterized with lesser h'F values as well as less steep change in the reduction of poleward wind velocities.

(4) During ESF days of vernal equinox, around ESF onset times, winds reduce their poleward magnitudes, thereby supporting ESF generation. This has been assisted by an increase in h'F values. Presence of relatively strong poleward winds during Autumn equinox as compared to Vernal equinox is noticed during ESF onset hours. This suggests that meridional winds may be one of the factors that may be causing equinoctial asymmetry wherein more number of ESF events are seen during Vernal equinox. Differences in solar flux could be another factor to be considered while studying the equinoctial differences in the wind. However during Summer (May-June-July), during 2000–2200 LT, wind velocities ranging from lesser poleward to equatorward can be noticed for ESF events. h'F values were less during these hours. However, non ESF days (May-Jul-Aug), shows increased poleward wind magnitudes around the period. During non ESF days, winds were more poleward during 2000–2200 LT. This was also supported by less h'F values. Winter season has strong poleward wind magnitudes than Autumn equinox cases during ESF days around their onset times. However, higher h'F values might have assisted the ESF generation during this period. In addition, although, h'F was high, stronger poleward velocities on non ESF days compared to ESF days might have resulted in ESF suppression.

(5) The FoF2 crest to trough ratio is seen slightly enhanced during ESF days than on non ESF days and the effect is seen to be more prominent during Winter and Summer solstice periods.

(6) Further, the observations indicate most probable combination of wind and h'F on ESF days are centered around 350 km and 50 m/s.

(7) Some case studies showed the presence of more equatorward winds, when lower PRE height is observed. Similarly, for larger poleward magnitudes, higher PRE height values might have conributed for ESF generation.This indicates the role of meridional winds on ESF occurrence during different PRE heights.

(8) Non scintillation days are characterized by the presence of larger poleward wind values during Vernal equinox and summer seasons than scintillation days. However, this trend is not visible during Autumn equinox seasons, where it is seen that meridional winds were poleward during both scintillation and non scintillation days. This might indicate the possible role of poleward meridional winds in reducing the number of scintillation occurences during this season in addition to weak PRE height.

Acknowledgements

This work is supported by Department of Science and Technology, Government of India. Also, we would like to thank the Director, IIG for providing necessary support. The authors gratefully acknowledge Suneel kumar Buduru, Scientist-in-Charge, TIFR Balloon facility, Hyderabad for providing Hyderabad ionosonde data. We would also like to thank K. Emperumal/C. Selvaraj, Equatorial Geophysical Research Laboratory, Tirunelveli for maintaining CADI ionosonde at Tirunelveli. The authors would also wish to acknowledge the use of MSISE-90 model which is obtained from http://omniweb.gsfc.nasa.gov/vitmo/msis_vitmo.html as well as HWM14 wind model. Authors also would like to thank the anonymous reviewers for their suggestions to improve the paper.

References

Abdu, M., 2005. Equatorial ionosphere–thermosphere system: electrodynamics and irregularities. Adv. Space Res. 35 (5), 771–787. http://dx.doi.org/10.1016/j.asr.2005.03.150.

Abdu, M., Iyer, K.N., de Medeiros, R., Batista, I.S., Sobral, J.H., 2006. Thermospheric meridional wind control of equatorial spread f and evening prereversal electric field. Geophys. Res. Lett. 33 (7). http://dx.doi.org/10.1029/2005GL024835.

Anderson, D., Rusch, D., 1980. Composition of the nighttime ionospheric f 1 region near the magnetic equator. J. Geophys. Res.: Space Phys. 85 (A2), 569–574. http://dx.doi.org/10.1029/JA085iA02p00569.

Banks, P., Kockarts, G., 1973. Aeronomy. Academic, New York.

Bittencourt, J., Abdu, M., 1981. A theoretical comparison between apparent and real vertical ionization drift velocities in the equatorial f region. J. Geophys. Res.: Space Phys. 86 (A4), 2451–2454. http://dx.doi.org/10.1029/JA086iA04p02451.

Chum, J., Liu, J.-Y., Chen, S.-P., Cabrera, M.A., Laštovička, J., Baše, J., Burešová, D., Fišer, J., Hruška, F., Ezquer, R., 2016. Spread f occurrence and drift under the crest of the equatorial ionization anomaly from continuous doppler sounding and formosat-3/cosmic scintillation data. Earth Planets Space 68 (1), 56. http://dx.doi.org/10.1186/s40623-016-0433-1.

de Abreu, A., Fagundes, P., Bolzan, M., de Jesus, R., Pillat, V., Abalde, J., Lima, W., 2014a. The role of the traveling planetary wave ionospheric disturbances on the equatorial f region post-sunset height rise during the last extreme low solar activity and comparison with high solar activity. J. Atmos. Sol.-Terrest. Phys. 113, 47–57. http://dx.doi.org/10.1016/j.jastp.2014.03.011.

de Abreu, A., Fagundes, P., Bolzan, M., Gende, M., Brunini, C., de Jesus, R., Pillat, V., Abalde, J., Lima, W., 2014b. Traveling planetary wave ionospheric disturbances and their role in the generation of equatorial spread-f and gps phase fluctuations during the last extreme low solar activity and comparison with high solar activity. J. Atmos. Sol.-Terrest. Phys. 117, 7–19. http://dx.doi.org/10.1016/j.jastp.2014.05.005.

Devasia, C., Jyoti, N., Subbarao, K., Viswanathan, K., Tiwari, D., Sridharan, R., 2002. On the plausible linkage of thermospheric meridional winds with the equatorial spread f. J. Atmos. Sol.-Terrest. Phys. 64 (1), 1–12. http://dx.doi.org/10.1016/S1364-6826(01)00089-X.

Drob, D.P., Emmert, J.T., Meriwether, J.W., Makela, J.J., Doornbos, E., Conde, M., Hernandez, G., Noto, J., Zawdie, K.A., McDonald, S.E., 2015. An update to the horizontal wind model (hwm): the quiet time thermosphere. Earth Space Sci. 2 (7), 301–319. http://dx.doi.org/10.1002/2014EA000089.

Hari, S., Murthy, B.K., 1995. Seasonal variations of equatorial night-time thermospheric meridional winds. J. Atmos. Terrest. Phys. 57 (11), 1241–1246.

Haridas, M.M., Manju, G., Arunamani, T., 2016. Solar activity variations of nocturnal thermospheric meridional winds over indian longitude sector. J. Atmos. Sol.-Terrest. Phys. 147, 21–27. http://dx.doi.org/10.1016/j.jastp.2016.06.010.

Huba, J., Krall, J., 2013. Impact of meridional winds on equatorial spread f: revisited. Geophys. Res. Lett. 40 (7), 1268–1272. http://dx.doi.org/10.1002/grl.50292.

Jyoti, N., Devasia, C., Sridharan, R., Tiwari, D., 2004. Threshold height (h? f) c for the meridional wind to play a deterministic role in the bottom side equatorial spread f and its dependence on solar activity. Geophys. Res. Lett. 31 (12). http://dx.doi.org/10.1029/2004GL019455.

Kelley, M., Larsen, M., LaHoz, C., McClure, J., 1981. Gravity wave initiation of equatorial spread f: a case study. J. Geophys. Res.: Space Phys. 86 (A11), 9087–9100.

Krishna Murthy, B., Hari, S., Somayajulu, V., 1990. Nighttime equatorial thermospheric meridional winds from ionospheric h'f data. J. Geophys. Res.: Space Phys. 95 (A4), 4307–4310. http://dx.doi.org/10.1029/JA095iA04p04307.

Kudeki, E., Akgiray, A., Milla, M., Chau, J.L., Hysell, D.L., 2007. Equatorial spread-f initiation: post-sunset vortex, thermospheric winds, gravity waves. J. Atmos. Sol.-Terrest. Phys. 69 (17), 2416–2427. http://dx.doi.org/10.1016/j.jastp.2007.04.012.

Liu, L., Luan, X., Wan, W., Lei, J., Ning, B., 2003. Seasonal behavior of equivalent winds over wuhan derived from ionospheric data in 2000–2001. Adv. Space Res. 32 (9), 1765–1770. http://dx.doi.org/10.1016/S0273-1177(03)90474-1.

Madhav Haridas, M., Manju, G., Pant, T.K., 2013. First observational evidence of the modulation of the threshold height h'fc for the occurrence of equatorial spread f by neutral composition changes. J. Geophys. Res.: Space Phys. 118 (6), 3540–3545. http://dx.doi.org/10.1002/jgra.50331.

Manju, G., Devasia, C., Sridharan, R., 2007. On the seasonal variations of the threshold height for the occurrence of equatorial spread f during solar minimum and maximum years. Annals Geophysicae, vol. 25, pp. 855–861.

Manju, G., Haridas, M.M., Aswathy, R., 2016. Role of gravity wave seed perturbations in esf day-to-day variability: a quantitative approach. Adv. Space Res. 57 (4), 1021–1028. http://dx.doi.org/10.1016/j.asr.2015.12.019.

Maruyama, T., 1988. A diagnostic model for equatorial spread f, 1, model description and application to electric field and neutral wind effects. J. Geophys. Res.: Space Phys. 93 (A12), 14611–14622. http://dx.doi.org/10.1029/JA093iA12p14611.

Maruyama, T., Matuura, N., 1984. Longitudinal variability of annual changes in activity of equatorial spread f and plasma bubbles. J. Geophys. Res.: Space Phys. 89 (A12), 10903–10912. http://dx.doi.org/10.1029/JA089iA12p10903.

Maruyama, T., Saito, S., Kawamura, M., Nozaki, K., 2008. Thermospheric meridional winds as deduced from ionosonde chain at low and equatorial latitudes and their connection with midnight temperature maximum. J. Geophys. Res.: Space Phys. 113 (A9). http://dx.doi.org/10.1029/2008JA013031.

Maruyama, T., Saito, S., Kawamura, M., Nozaki, K., Krall, J., Huba, J., 2009. Equinoctial asymmetry of a low-latitude ionosphere-thermosphere system and equatorial irregularities: evidence for meridional wind control. Annals Geophysicae, vol. 27. Copernicus, GmbH, pp. 2027–2034. http://dx.doi.org/10.5194/angeo-27-2027-2009.

Muella, M.T.d.A.H., de Paula, E., Fagundes, P., Bittencourt, J., Sahai, Y., 2010. Thermospheric meridional wind control on equatorial scintillations and the role of the evening f-region height rise, e× b drift velocities and f2-peak density gradients. Surv. Geophys. 31 (5), 509–530. http://dx.doi.org/10.1007/s10712-010-9101-3.

Oyekola, O., 2009. A study of evolution/suppression parameters of equatorial postsunset plasma instability. Annals Geophysicae, vol. 27. Copernicus, GmbH, pp. 297–301. http://dx.doi.org/10.5194/angeo-27-297-200.

Raghavarao, R., Hoegy, W., Spencer, N., Wharton, L., 1993. Neutral temperature anomaly in the equatorial thermosphere-a source of vertical winds. Geophys. Res. Lett. 20 (11), 1023–1026. http://dx.doi.org/10.1029/93GL01253.

Raghavarao, R., Nageswararao, M., Sastri, J.H., Vyas, G., Sriramarao, M., 1988. Role of equatorial ionization anomaly in the initiation of equatorial spread f. J. Geophys. Res.: Space Phys. 93 (A6), 5959–5964. http://dx.doi.org/10.1029/JA093iA06p05959.

Rishbeth, H., Ganguly, S., Walker, J., 1978. Field-aligned and field-perpendicular velocities in the ionospheric f2-layer. J. Atmos. Terrest. Phys. 40 (7), 767–784. http://dx.doi.org/10.1016/0021-9169(78)90028-4, 30.

Sekar, R., Sridharan, R., 1992. Validity of the estimates of night-time meridional winds made from bottomside ionograms. J. Atmos. Terrest. Phys. 54 (9), 1197–1199. http://dx.doi.org/10.1016/0021-9169(92)90144-A.

Sreeja, V., Devasia, C., Ravindran, S., Sridharan, R., 2009. The persistence of equatorial spread f–an analysis on seasonal, solar activity and geomagnetic activity aspects. Annals Geophysicae, vol. 27. Copernicus, GmbH, pp. 503–510. http://dx.doi.org/10.5194/angeo-27-503-200.

Sreekumar, S., Sripathi, S., 2016. Nighttime thermospheric meridional winds as inferred from ionosonde parameters over indian region and their plausible effects on plasma irregularities. Adv. Space Res. 58 (1), 92–107. http://dx.doi.org/10.1016/j.asr.2016.04.009.

Sridharan, R., Bagiya, M.S., Sunda, S., Choudhary, R., Pant, T.K., Jose, L., 2014. First results on forecasting the spatial occurrence pattern of l-band scintillation and its temporal evolution. J. Atmos. Sol.-Terrest. Phys. 119, 53–62. http://dx.doi.org/10.1016/j.jastp.2014.06.015.

Sripathi, S., Kakad, B., Bhattacharyya, A., 2011. Study of equinoctial asymmetry in the equatorial spread f (esf) irregularities over indian region using multi-instrument observations in the descending phase of solar cycle 23. J. Geophys. Res.: Space Phys. 116 (A11). http://dx.doi.org/10.1029/2011JA016625.

Sultan, P., 1996. Linear theory and modeling of the rayleigh-taylor instability leading to the occurrence of equatorial spread f. J. Geophys. Res.: Space Phys. 101 (A12), 26875–26891. http://dx.doi.org/10.1029/96JA00682.

Valladares, C., Meriwether, J., Sheehan, R., Biondi, M., 2002. Correlative study of neutral winds and scintillation drifts measured near the magnetic equator. J. Geophys. Res.: Space Phys. 107 (A7). http://dx.doi.org/10.1029/2001JA000042.